them for degradation. Finally, our study suggests a role for Mdm2 sequences distinct from those required for p53 binding, in targeting proteins for degradation, suggesting that other Mdm2-associated proteins, such as RB and E2F, may also be destabilized as a result of the interaction with Mdm2, or may modify the stability of p53 through their interaction with Mdm2. □

Methods

Plasmids, antibodies and proteasome inhibitor. Plasmids encoding mouse wild-type Mdm2 (pCOC Mdm2 X2)[5], human wild-type Mdm2 (pCHDM), human mutant Mdm2 Δ222–437 (pCHDM Δ222–437)[6], human wild-type p53 (pCB6 + p53Pro) and mutant p53 (pCB6 + p53ΔI (ref. 13), pcB6 + Ala15, pCB6 + Asp15 (ref. 28) and pCMV p53 22/23 (ref. 14)) under the control of the CMV promoter have been described previously. p53-specific monoclonal antibodies PAb1801, D0-1 and PAb421 and the Mdm2-specific antibody IF2 were purchased from Oncogene Science. The polyclonal rabbit serum CM-1 was from Novocastra. The proteasome inhibitor lactacystin was purchased from E. J. Corey.

Cells and transfections. Saos-2 (p53 null), U2OS (p53 wild type), C33A (p53 mutant) cells, and *p53*-null and *p53/mdm2* double-null mouse embryo fibroblasts (MEF) were maintained in DMEM supplemented with 10 or 15% fetal calf serum, respectively, and transiently transfected using the calcium phosphate precipitation method. Unless otherwise indicated, 1 μg wild-type *p53* or mutant *p53* plasmid were cotransfected with 2 μg Mdm2-encoding plasmid per 60-mm dish and cells were collected 24 h after transfection. Where appropriate, transfection efficiency was verified by cotransfection of 1.5 μg of CMV-driven β-galactosidase expression plasmid and measurement of enzymatic β-galactosidase activity. For studies of endogenous p53 levels, cells were cotransfected with 1.5 μg pHook and 1.5 μg β galactosidase expression plasmid and transfected cells were separated from untransfected cells using the Capture-Tec kit (Clontech).

Protein analysis. Western blotting, immunoprecipitation[29] and flow cytometry[30] for p53 protein were carried out as previously described. Equal loading of total protein was confirmed by Ponceau S staining. For pHook-selected cells, lysates were normalized for β-galactosidase activity. The stability of p53 protein in transfected cells was determined by radioactive pulse labelling of cells for 1 h and chase in unlabelled medium for 0, 1, 3, 6 and 12 h followed by immunoprecipitation of p53 using monoclonal antibody PAb421. Quantification of labelled p53 protein was carried out using the STORM phosphoimager 860 (Molecular Dynamics).

Northern blot analysis. For northern blotting, full-length p53 cDNA was used as p53 probe; the β-actin probe was obtained from Clontech.

Received 2 January; accepted 3 April 1997.

1. Bates, S. & Vousden, K. H. p53 in signalling checkpoint arrest or apoptosis. *Current Opin. Genet. Dev.* **6,** 1–7 (1996).
2. Barak, Y. & Oren, M. Enhanced binding of a 95 kDa protein to p53 in cells undergoing p53-mediated growth arrest. *EMBO J.* **11,** 2115–2121 (1992).
3. Momand, J., Zambetti, G. P., George, D. L. & Levine, A. J. The mdm-2 oncogene product forms a complex with the p53 protein and inhibits p53-mediated transactivation. *Cell* **69,** 1237–1245 (1992).
4. Chen, J. D., Marechal, V. & Levine, A. J. Mapping of the p53 and mdm-2 interaction domains. *Mol. Cell. Biol.* **13,** 4107–4114 (1993).
5. Haupt, Y., Barak, Y. & Oren, M. Cell type-specific inhibition of p53-mediated apoptosis by mdm2. *EMBO J.* **15,** 1596–1606 (1996).
6. Chen, J., Wu, X., Lin, J. & Levine, A. J. mdm-2 inhibits the G1 arrest and apoptosis functions of the p53 tumor suppressor protein. *Mol. Cell. Biol.* **16,** 2445–2452 (1996).
7. Barak, Y., Juven, T., Haffner, R. & Oren, M. mdm-2 expression is induced by wild type p53 activity. *EMBO J.* **12,** 461–468 (1993).
8. Wu, X. W., Bayle, J. H., Olson, D. & Levine, A. J. The p53 mdm-2 autoregulatory feedback loop. *Genes Dev.* **7,** 1126–1132 (1993).
9. Montes de Oca Luna, R., Wagner, D. S. & Lozano, G. Rescue of early embryonic lethality in *mdm2*-deficient mice by absence of p53. *Nature* **378,** 203–206 (1995).
10. Jones, S. N., Roe, A. E., Donehower, L. A. & Bradley, A. Rescue of embyonic lethality in Mdm2-deficient mice by absence of p53. *Nature* **378,** 206–208 (1995).
11. Xiao, Z.-X. *et al.* Interaction between the retinoblasmoma protein and the oncoprotein MDM2. *Nature* **375,** 694–697 (1995).
12. Martin, K. *et al.* Stimulation of E2F1/DP1 transcriptional activity by MDM2 oncoprotein. *Nature* **375,** 691–694 (1995).
13. Marston, N. J., Crook, T. & Vousden, K. H. Interaction of p53 with MDM2 is independent of E6 and does not mediate wild type transformation suppressor function. *Oncogene* **9,** 2707–2716 (1994).
14. Lin, J., Chen, J., Elenbaas, B. & Levine, A. J. Several hydrophobic amino acids in the p53 amino-terminal domain are required for transcriptional activation, binding to mdm-2 and the adenovirus 5 E1B 55-kD protein. *Genes Dev.* **8,** 1235–1246 (1994).
15. Lees-Miller, S. P., Sakaguchi, K., Ullrich, S. J., Appella, E. & Anderson, C. W. Human DNA-activated protein kinase phosphorylates serines 15 and 37 in the amino-terminal transactivation domain of human p53. *Mol. Cell. Biol.* **12,** 5041–5049 (1992).
16. Scheffner, M., Werness, B. A., Huibregtse, J. M., Levine, A. J. & Howley, P. M. The E6 oncoprotein encoded by human papillomavirus types 16 and 18 promotes the degradation of p53. *Cell* **63,** 1129–1136 (1990).
17. Hubbert, N. L., Sedman, S. A. & Schiller, J. T. Human papillomavirus type 16 E6 increases the degradatin rate of p53 in human keratinocytes. *J. Virol.* **66,** 6237–6241 (1992).
18. Jones, S. N. *et al.* The tumorigenic potential and cell growth characteristics of p53-deficient cells are equivalent in the presence or absence of Mdm2. *Proc. Natl Acad. Sci. USA* **93,** 14106–14111 (1996).
19. Wrede, D., Tidy, J. A., Crook, T., Lane, D. & Vousden, K. H. Expression of RB and p53 proteins in HPV-positive and HPV-negative cervical carcinoma cell lines. *Mol. Carcinog.* **4,** 171–175 (1991).
20. Maki, C. G., Huibregtse, J. & Howley, P. M. *In vivo* ubiquitination and proteosome-mediated degradation of p53. *Cancer Res.* **56,** 2649–2654 (1996).
21. Kubbutat, M. H. G. & Vousden, K. H. Proteolytic cleavage of human p53 by calpain: a potential regulator of protein stability. *Mol. Cell. Biol.* **17,** 460–468 (1997).
22. Fenteany, G. *et al.* Inhibition of proteasome activities and subunit-specific amino-terminal threonine modification by lactacytin. *Science* **268,** 726–731 (1995).
23. Oliner, J. D. *et al.* Oncoprotein MDM2 conceals the activation domain of tumour suppressor p53. *Nature* **362,** 857–860 (1993).
24. Haupt, Y., Maya, R., Kazaz, A. & Oren, M. Mdm2 promotes the rapid degradation of p53. *Nature* **387,** 296–299 (1997).
25. Di Leonardo, A., Linke, S. P., Clarkin, K. & Wahl, G. M. DNA damage triggers a prolonged p53-dependent G1 arrest and long-term induction of Cip1 in normal human fibroblasts. *Genes Dev.* **8,** 2540–2551 (1994).
26. Perry, M. E., Piette, J., Zawadzki, J. A., Harvey, D. & Levine, A. J. The mdm-2 gene is induced in response to UV light in a p53-dependent manner. *Proc. Natl Acad. Sci. USA* **90,** 11623–11627 (1993).
27. Chen, C. Y. *et al.* Interactions between p53 and MDM2 in a mammalian cell cycle checkpoint pathway. *Proc. Natl Acad. Sci. USA* **91,** 2684–2688 (1994).
28. Marston, N. J. *Mutational Analysis of the Tumour Suppressor Protein p53.* Thesis, Univ. London (1996).
29. Marston, N. J., Jenkins, J. R. & Vousden, K. H. Oligomerisation of full length p53 contributes to the interaction with mdm2 but not HPV E6. *Oncogene* **10,** 1707–1715 (1995).
30. Rowan, S. *et al.* Specific loss of apoptotic but not cell cycle arrest function in a human tumour derived p53 mutant. *EMBO J.* **15,** 827–838 (1996).

Acknowledgements. We thank D. Lane, B. Vogelstein, A. Levine and M. Oren for gifts of plasmids and antibodies; M. Oren and Y. Haupt for discussion and sharing unpublished data; and S. Bates and A. Phillips for reading the manuscript. This work was supported by the National Cancer Institute, DHHS, under contract with ABL.

Correspondence and requests for materials should be addressed to K.H.V. (e-mail: vousden@ncifcrf.gov).

Regulation of serotonin-2C receptor G-protein coupling by RNA editing

Colleen M. Burns, Hsin Chu, Susan M. Rueter, Linda K. Hutchinson, Hervé Canton, Elaine Sanders-Bush & Ronald B. Emeson

Department of Pharmacology, Vanderbilt University School of Medicine, Nashville, Tennessee 37232-6600, USA

The neurotransmitter serotonin (5-hydroxytryptamine, 5-HT) elicits a wide array of physiological effects by binding to several receptor subtypes. The 5-HT_2 family of receptors belongs to a large group of seven-transmembrane-spanning G-protein-coupled receptors and includes three receptor subtypes (5-HT_{2A}, 5-HT_{2B} and 5-HT_{2C}) which are linked to phospholipase C, promoting the hydrolysis of membrane phospholipids and a subsequent increase in the intracellular levels of inositol phosphates and diacylglycerol[1]. Here we show that transcripts encoding the 2C subtype of serotonin receptor (5-HT_{2C}R) undergo RNA editing events in which genomically encoded adenosine residues are converted to inosines by the action of double-stranded RNA adenosine deaminase(s). Sequence analysis of complementary DNA isolates from dissected brain regions have indicated the tissue-specific expression of seven major 5-HT_{2C} receptor isoforms encoded by eleven distinct RNA species. Editing of 5-HT_{2C}R messenger RNAs alters the amino-acid coding potential of the predicted second intracellular loop of the receptor and can lead to a 10–15-fold reduction in the efficacy of the interaction between receptors and their G proteins. These observations indicate that RNA editing is a new mechanism for regulating serotonergic signal transduction and suggest that this post-transcriptional modification may be critical for modulating the different cellular functions that are mediated by other members of the G-protein-coupled receptor superfamily.

Sequence analysis of clones isolated from a rat striatum cDNA library predicted the presence of valine (GTG), serine (AGT) and valine (GTT) codons within the second intracellular loop of the 5-HT_{2C}R; instead, isoleucine (ATA), asparagine (AAT) and isoleucine (ATT) codons were found in the genomic DNA sequence at these positions (Fig. 1a). The A-to-G nucleotide discrepancies at these positions (termed sites A, B, C and D) were similar to those identified in the RNA editing of transcripts encoding the hepatitis delta virus antigenome and subunits of the α-amino-3-hydroxy-5-methyl-4-isoxazolepropionic acid (AMPA) and kainate subtypes of ionotropic glutamate receptors[2–6].

To investigate whether the nucleotide differences in 5-HT_{2C}R transcripts resulted from a similar RNA editing process, a 3.2-kilobase (kb) rat 5-HT_{2C}R genomic fragment containing exon 3 and the proximal region of the third intron was expressed transiently in the rat C6 glioma cell line (Fig. 1b, left). Primer-extension analysis of pre-mRNA derived from the transfected minigene identified A → G conversions at the A, C and D sites, showing that the A → G nucleotide discrepancies between genomic and cDNA sequences resulted from the post-transcriptional editing of 5-HT_{2C}R transcripts (Fig. 1b, right). Subsequent sequence analysis of reverse transcription–polymerase chain reaction (RT-PCR) products derived from 5-HT_{2C}R pre-mRNA transcripts confirmed the presence of similar A → G discrepancies for the B editing site (data not shown). Transient expression of 5-HT_{2C}R minigenes containing progressively smaller portions of intron 3 indicated that efficient editing could be achieved using an RNA transcript containing only 288 nucleotides of sequence information (Fig. 1b). Transcripts derived from a cDNA fragment extending from exon 3 through exon 4 (377 nucleotides)had background levels of editing at all sites, suggesting that the *cis*-active element(s) necessary for 5-HT_{2C}R editing included sequences in the proximal region of the third intron. Further analysis of pre-mRNA sequences using RNA folding algorithms[7] identified an imperfect inverted repeat forming a putative RNA duplex between the 3′ end of exon 3 and the proximal region of intron 3 (Fig. 1c). Introduction of mutations to disrupt proposed RNA base pairing abolished editing at all four sites, whereas introduction of compensatory sequence alterations restored editing to wild-type levels (data not shown). These results show that the editing of 5-HT_{2C}R transcripts requires the presence of an RNA duplex structure, similar to that previously identified for RNAs encoding AMPA and kainate glutamatergic receptor subunits[4,8,9].

To examine further the molecular mechanisms by which 5-HT_{2C}R transcripts are post-transcriptionally modified, an *in vitro* 5-HT_{2C}R editing system[10,11] was developed using rat brain nuclear extracts fractionated by cation-exchange chromatography and a 5-HT_{2C}R RNA substrate (288 nucleotides; Fig. 1b) uniformly labelled with [α-^{32}P]adenosine 5′-triphosphate. Thin-layer chromatography of *in vitro* reaction products revealed two peaks of inosine (rather than guanosine) produced from radiolabelled 5-HT_{2C}R substrate (Fig. 2a); these activities co-eluted with two distinct peaks of double-stranded RNA (dsRNA)-adenosine deaminase activity which was detected upon incubation of fractionated extracts with

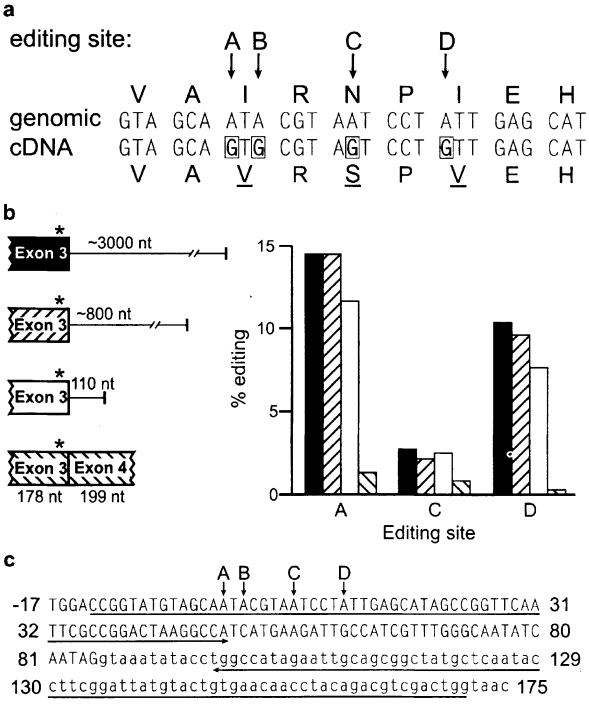

Figure 1 RNA editing of 5-HT_{2C}R transcripts. **a**, Nucleotide and predicted amino-acid sequence alignments between 5-HT_{2C}R genomic and cDNA sequences; A → G nucleotide discrepancies and predicted alterations in amino acid sequence are indicated by boxed and underlined letters, respectively. The positions of four putative editing sites (A, B, C and D) are indicated. **b**, 5-HT_{2C}R minigene transcription units: editing sites (asterisk), lengths of introns (lines) and exons (boxes), and the efficiency of editing for each site upon transient transfection into rat C6 glioma cells are indicated. **c**, Nucleotide sequence of 5-HT_{2C}R genomic DNA in the proximal region of intron 3. The positions of the editing sites are indicated and an imperfect inverted repeat is shown with underlying arrows. Intronic sequence information is designated by lower-case letters and coordinates are relative to the A-site at position 0.

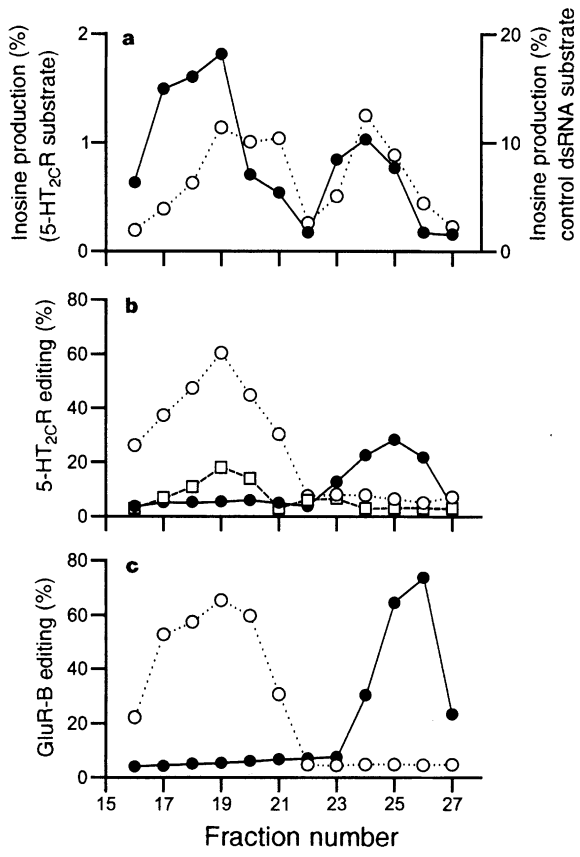

Figure 2 Chromatography of rat brain RNA-editing activity. **a**, *In vitro* production of inosine from [α-^{32}P]ATP labelled 5-HT_{2C}R RNA (●) or synthetic α_{2A} adrenergic receptor dsRNA (○) substrates incubated with rat brain nuclear extract fractionated by cation-exchange chromatography. **b**, Elution profile of site-specific 5-HT_{2C}R editing activity at the A (○), C (□) and D (●) sites. **c**, Elution profile of site-specific GluR-B editing activity at the +60 (○), and Q/R (●) sites.

a control dsRNA substrate. Primer-extension analysis of 5-HT_{2C}R *in vitro* reaction products identified two RNA editing activities (Fig. 2b) which co-eluted with the dsRNA-adenosine deaminase peaks (Fig. 2a). The first peak of activity was responsible for editing 5-HT_{2C}R transcripts at the A, C (Fig. 2b) and B (data not shown) sites and co-eluted with the activity mediating the modification of RNAs encoding the B-subunit of the AMPA subtype of glutamate receptor (GluR-B) at intronic position +60 (Fig. 2c). The second peak of activity specifically modified the D site of 5-HT_{2C}R transcripts (Fig. 2b) and the Q/R site of GluR-B (Fig. 2c). These results suggest that the editing of 5-HT_{2C}R transcripts *in vitro* is mediated by the actions of two separable double-stranded RNA adenosine deaminases, similar to that described for GluR-B RNAs[11,12], and further suggest that the editing of both 5-HT_{2C}R and GluR-B transcripts is mediated by a common cellular machinery.

Previous studies using tissue culture and *in vitro* model systems have suggested that dsRNA-specific adenosine deaminase (dsRAD or DRADA) is responsible for the modification of GluR-B transcripts at intronic position +60 (refs 12, 13), whereas dsRNA-specific editase 1 (RED1) is more selective for the Q/R site[13]. To test whether these enzymes could mediate the site-specific modification of 5-HT_{2C}R transcripts, human embryonic kidney cells (HEK293) were transiently co-transfected with a 288-nucleotide 5-HT_{2C}R minigene construct and either a rat dsRAD/DRADA or RED1 cDNA clone. Primer-extension analysis (Fig. 3a, b) of RNA transcripts derived from the transfected minigene, in the absence of exogenous dsRAD/DRADA or RED1, revealed minimal editing at all positions (Fig. 3c, d), consistent with previous observations that HEK293 cells contain a low endogenous GluR-B editing activity[12,13]. Co-expression of dsRAD/DRADA led to a significant increase in editing efficiency at the A and C sites but had little effect upon modification of the D site. RED1 expression, by contrast, led to a significant increase in editing at all three sites, although the effects were most dramatic for the D site (Fig. 3c, d). These results show that dsRAD/DRADA and RED1 can selectively modify 5-HT_{2C}R transcripts and that these dsRNA-specific adenosine deaminases may mediate the editing of both GluR-B and 5-HT_{2C}R pre-mRNAs. Discrepancies between the site selectivity using *in vitro* editing (Fig. 2b) rather than co-transfection (Fig. 3) strategies could result from differences in enzyme activity or from requirements for additional regulatory factors.

Although edited 5-HT_{2C}R mRNAs were initially identified in rat striatum, the potential role of dsRAD/DRADA and RED1 in 5-HT_{2C}R editing and the broad expression patterns demonstrated by these enzymes have suggested that edited 5-HT_{2C}R mRNAs could be widely distributed throughout the central nervous system[13,14]. Primer extension and dideoxynucleotide sequence analyses of 5-HT_{2C}R mRNA derived from dissected brain regions revealed a tissue-specific pattern for these post-transcriptional modifications (Fig. 4), with the choroid plexus (the site of greatest 5-HT_{2C}R production) expressing relatively few transcripts edited at the A and

Table 1 Quantitative analysis of region-specific 5-HT_{2C}R isoform expression

Amino-acid isoforms	RNA isoforms	Whole brain	Hippocampus	Choroid plexus
VNV	ABD AD	47	36	6
VNI	AB A	18	20	0
VSV	ABCD ACD	11	22	10
VSI	ABC AC	10	18	2
INV	D	5	0	38
ISV	CD	1	0	20
INI		2	0	18

RNAs from whole rat brain, hippocampus and choroid plexus were amplified by RT-PCR and subcloned into pBKSII$^-$; individual cDNA isolates were sequenced. The number of individually sequenced cDNA isolates were 100, 50 and 50 for whole brain, hippocampus and choroid plexus, respectively. 5-HT_{2C}R RNA isoforms, and the corresponding amino-acid variants predicted by them, are indicated. Numbers represent the percentage of cDNA isolates encoding each amino-acid isoform.

d

Editing site	Editing (%)		
	Control	RED1	dsRAD/DRADA
A	8.6 ± 1.3	26.1 ± 3.7	63.4 ± 8.1
C	4.7 ± 2.3	40.3 ± 6.7	25.8 ± 5.1
D	1.5 ± 0.8	75.8 ± 8.3	3.1 ± 0.3

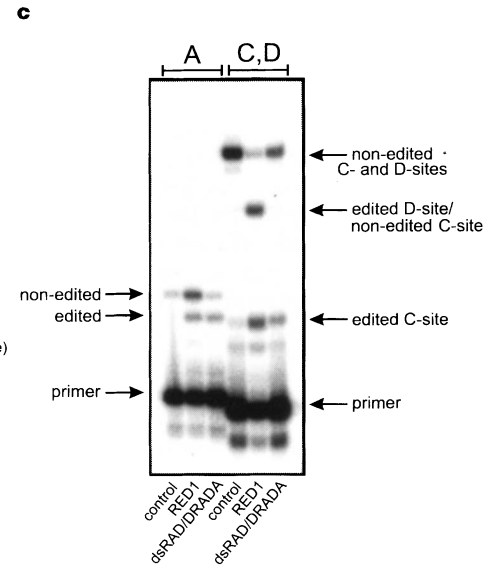

Figure 3 Co-transfection analysis of 5-HT_{2C}R transcripts and recombinant dsRNA-specific adenosine deaminases. **a**, Primer-extension strategy for quantification of editing at the 5-HT_{2C}R A-site. The nucleotide sequence of a 5′-end-labelled (asterisk) oligonucleotide sense primer, the antisense strand of the RT-PCR template, the positions of the editing sites and the sequences of expected primer-extension products are indicated. **b**, Primer-extension strategy for quantification of editing at the 5-HT_{2C}R C- and D-sites. Degenerate positions within the radiolabelled primer are indicated with an R (purine). **c**, RT-PCR/primer-extension analysis of total RNA isolated from HEK 293 cells transiently co-transfected with a 288-bp 5-HT_{2C}R genomic construct and dsRAD/DRADA or RED1 cDNA clones. The migration positions of the primers and edited and non-edited extension products are indicated. **d**, Quantification of 5-HT_{2C}R primer-extension analysis indicating editing efficiencies at the A, C and D sites in the presence or absence of dsRAD/DRADA or RED1; values represent the mean (±standard deviation), $n = 3$.

B sites compared with other areas examined. Sequence analyses of individual cDNA isolates derived from dissected brain regions predicted the presence of seven major 5-HT_{2C}R isoforms encoded by 11 RNA species (Table 1). The most common 5-HT_{2C}R variant in whole brain and hippocampus was encoded primarily by editing at the A, B and D sites, predicting the expression of a protein isoform containing valine, asparagine and valine (VNV) at the relevant positions. The VSV, VNI and VSI variants also comprised a substantial percentage of the receptor RNAs isolated from these tissues. In contrast, the choroid plexus expressed relatively few RNA molecules encoding these isoforms owing to the reduced editing at the A and B sites (Fig. 4), and instead expressed large amounts of the INV, ISV and INI isoforms. Nine additional RNA species were also identified, but in general they represented less than 2% of the total 5-HT_{2C}R transcripts.

The observation that choroid plexus editing patterns were significantly different from those seen in other brain regions suggested that differentially edited 5-HT_{2C} receptors may have distinct biological functions in those regions in which they are expressed. As RNA editing alters the primary amino-acid sequence in the second intracellular loop of the 5-HT_{2C} receptor, a region implicated in receptor–G-protein (R-G) coupling[15], early analyses of receptor function focused upon activation of phospholipase C and the subsequent accumulation of inositol phosphates. The fully edited VSV and unedited INI 5-HT_{2C}R isoforms were transiently transfected into NIH3T3 fibroblasts and assayed for 5-HT-stimulated inositol phosphate (InsP) accumulation. Both receptors were coupled to activation of phosphoinositide hydrolysis, but comparison of the 5-HT dose–response curve demonstrated that the agonist was 10–15-fold less potent in cells expressing the VSV isoform than the wild-type 5-HT_{2C}R (Fig. 5a). Possible explanations for this difference in 5-HT potency include alterations in the intrinsic affinity of the receptor, desensitization kinetics, spare receptors, and the efficacy of R-G coupling.

The affinity for 5-HT and (−)DOB[(−)1-(4-bromo-2,5-dimethoxyphenyl)-2-aminopropane], determined by competition binding, was nearly equal for the INI and VSV 5-HT_{2C}R isoforms, showing that the different potency does not result from an altered agonist affinity (Fig. 5b). This idea was substantiated by antagonist competition binding, in which a series of antagonists (clozapine, ketanserin, mesulergine, bromolysergic acid diethylamide (bromo-LSD), mianserin) had similar affinities for both receptor isoforms (Fig. 5b). Desensitization of 5-HT_{2C}R receptors has also been associated with a reduced potency for 5-HT, but InsP formation in the presence of 5-HT is linear with the VSV variant for at least 30 min (data not shown), as shown for the wild-type 5-HT_{2C}R receptor[16]. The lower half-maximal effective concentration(EC_{50}) values determined for certain receptor isoforms (that is, the wild-type receptor) could also be explained by the presence of spare receptors, in which full receptor occupancy is not required for maximal phosphoinositide hydrolysis[17]. To test this, an alkylating agent (phenoxybenzamine, PBZ) was used to inactivate a fraction of the 5-HT_{2C} receptors before analysis of 5-HT-stimulated InsP accumulation (Fig. 5c)[18]. The absence of spare receptors is reflected by the ability of phenoxybenzamine to decrease the maximal response of the wild-type 5-HT_{2C}R (INI) without affecting 5-HT potency. A comparable decrease in maximal response to 5-HT, with no shift in potency, was found after treatment of the VSV isoform with PBZ (data not shown). We conclude that the decreased potency of 5-HT for activating phosphoinositide hydrolysis, upon stimulation of the VSV receptor isoform, reflects reduced R-G coupling. The usual indirect methods for assessing R-G coupling, such as GTP-induced shifts in agonist affinity, agonist-promoted GTP-γS binding or GTPase activity, produce low or non-existent signals with 5-HT_{2C} receptors and are therefore not useful for studying R-G coupling efficiency in 5-HT_{2C}R isoforms[19]. These methods are generally not adequate for receptors coupled to the Gq family of G proteins and may reflect a low intrinsic GTP-turnover rate[20].

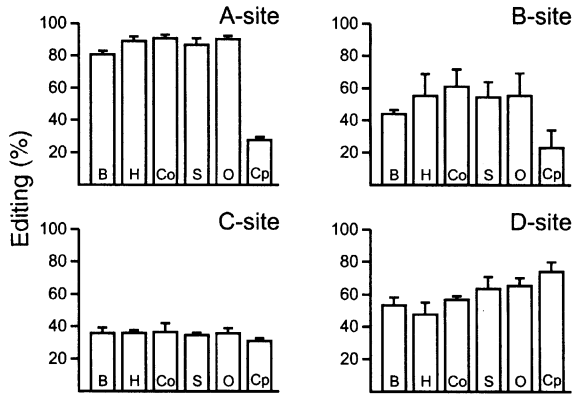

Figure 4 Analysis of site-specific 5-HT_{2C}R editing patterns. The percentage A → G conversion (editing efficiency) for each editing site (A, B. C, D) is presented for whole rat brain and dissected brain regions. Error bars represent the standard deviation from at least three independent experiments. Whole rat brain, B; hippocampus, H; cortex, Co; striatum, S; olfactory bulb, O; choroid plexus, Cp.

To define the specific amino-acid alterations responsible for decreased R-G coupling, individual 5-HT_{2C}R isoforms were transiently transfected in NIH3T3 fibroblasts and assessed for 5-HT-stimulated InsP accumulation (Fig. 5d). The results indicated that only fully edited receptor isoforms, encoding a valine, serine and valine (VSV) at positions 157, 159 and 161, respectively, exhibited reduced R-G coupling. Receptor isoforms with asparagine or isoleucine at these positions demonstrated equal 5-HT potencies as the non-edited INI receptor.

We have demonstrated that pre-mRNAs encoding the 5-HT_{2C} receptor are post-transcriptionally modified by dsRNA-adenosine deaminase(s) to yield multiple 5-HT_{2C}R transcripts. The cellular machinery mediating these modifications is similar (or identical) to that described for RNAs encoding ionotropic glutamate receptor subunits, and may involve the enzymes dsRAD/DRADA and RED1 (refs 10–13). Region-specific editing of 5-HT_{2C}R transcripts generates multiple receptor isoforms, one of which (VSV) couples less efficiently to the intracellular signalling machinery, representing a new mechanism for regulating serotonergic signal transduction. Region- or cell-specific differences in the production of 5-HT_{2C}R isoforms may represent a stochastic event or a dynamically regulated process that modulates receptor activity thereby altering cellular responses to ambient levels of neurotransmitter. Mutagenesis of the muscarinic cholinergic receptor has shown that amino-acid residues within the conserved second intracellular loop sequence DRYXXV(I)XXPL are critical for maintaining optimal R-G interactions[21], consistent with our evidence that editing in this region reduces the efficacy of R-G coupling. Possible explanations for this reduced R-G coupling in the fully edited 5-HT_{2C}R isoform (VSV) include altered receptor structure or receptor phosphorylation at the introduced serine moiety. Sequence analysis of mouse 5-HT_{2C}R indicates that Ser 159 may represent a potential casein kinase II site[22], although amino-acid residues in this region do not strongly conform to phosphorylation consensus sequences[23]. To our knowledge, the 5-HT_{2C}R is the first G-protein-coupled receptor to be regulated by RNA editing, suggesting that similar post-transcriptional modifications may modulate the different cellular responses mediated by other G-protein-coupled receptors. □

Methods

Isolation of cDNA clones. A cDNA library generated from rat striatum (λ-ZAPII; Stratagene) was screened using a randomly primed *Msc*I–*Age*I fragment

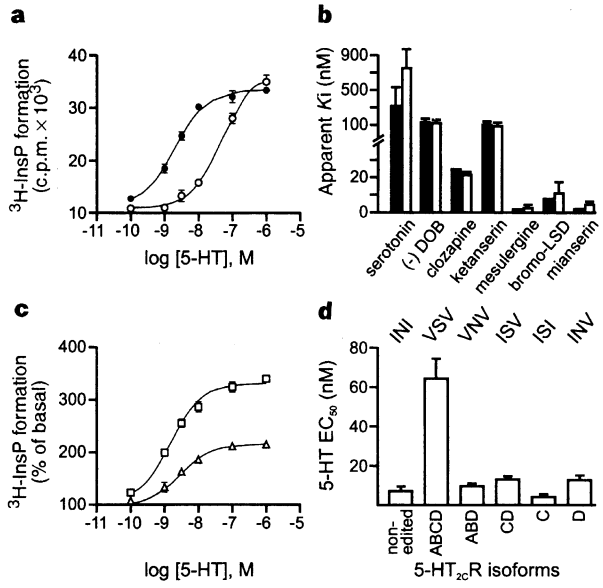

Figure 5 Functional analysis of 5-HT$_{2C}$R isoforms. **a**, Effect of serotonin on [^{3}H]-InsP formation in NIH 3T3 fibroblasts transiently transfected with cDNA encoding INI (●) or VSV (○) 5-HT$_{2C}$R isoforms; B_{max} and EC_{50} values were 5,387 versus 5,362 fmol per mg protein and 2 versus 40 nM for the INI and VSV isoforms, respectively. **b**, Apparent K_i values of agonists and antagonists for INI (filled boxes) and VSV (open boxes) 5-HT$_{2C}$R isoforms. **c**, Effect of phenoxybenzamine (PBZ) on 5-HT-elicited phosphoinositide hydrolysis in NIH3T3 fibroblasts transiently expressing the 5-HT$_{2C}$R (INI) isoform. Transfected cells were treated with either vehicle (□) or 1.6 μM PBZ (△) for 30 min before analysis. **d**, Potencies of 5-HT in eliciting [^{3}H]-IP accumulation in NIH3T3 cells expressing 5HT$_{2C}$R variants. All data were analysed by nonlinear regression and values represent the mean (±s.e.); **a**, $n = 10$; **b**, $n = 3$–6; **c**, $n = 3$; **d**, $n = 4$–18.

corresponding to positions 856–1,143 of the rat 5-HT$_{2C}$R cDNA sequence as described[24,25]. The nucleotide sequence of exon 3 was compared to the corresponding sequence of a rat 5-HT$_{2C}$R genomic clone obtained from Genome Systems (St Louis, MO). Seven cDNA clones were isolated with various combinations of A to G discrepancies at the A, B, C and D editing sites.

A rat dsRAD/DRADA cDNA clone was obtained by screening a whole rat brain cDNA library (λ-ZAPII) with a randomly primed probe generated from a 606-bp fragment of human dsRAD/DRADA corresponding to position 1,812–2,417 as described[26]. The isolated 4.1-kb rat cDNA clone contained the entire dsRAD/DRADA coding region with 44 and ~500 bp of 5′ and 3′ untranslated information, respectively.

A 2.3-kb rat RED1 cDNA clone was obtained by RT-PCR amplification of whole rat brain total RNA using sense and antisense oligonucleotide primers corresponding to positions 12–35 and 2,311–2,333 of the rat RED1 sequence[13].

Tissue culture and transfection studies. For transfection studies (Figs 1 (C6, rat glioma) and 3 (HEK 293, human embryonic kidney)), 5-HT$_{2C}$R genomic fragments, as well as dsRAD/DRADA and RED1 cDNAs, were subcloned into the eukaryotic expression vector pRC/CMV (Invitrogen) and transiently expressing cells were established using calcium phosphate coprecipitation[25]. RNAs were prepared ~60 h after transfection and editing at the A, C and D sites was analysed by primer extension. For transient transfections of 5-HT$_{2C}$R cDNA isoforms (Fig. 5), NIH3T3 cells (90% confluence) were trypsinized, rinsed and suspended in OPTI-MEMI (Gibco-BRL) at 25×10^6 cells ml^{-1} one hour before electroporation. 10–30 μg 5-HT$_{2C}$R isoform plasmid DNA (in the eukaryotic expression vector pCMV2) was mixed with cell suspension (10×10^6 cells) in a sterile electroporation cuvette and an electric pulse (270 V, 950 mF) was applied (Bio-Rad Gene Pulser II).

Quantification of editing efficiency. Total RNA from tissue culture cells or dissected brain areas was prepared by the guanidinium-isothiocyanate method[25]. For analysis of the transfected 5-HT$_{2C}$R minigene constructs (Fig. 1b), reverse transcription was done with an oligonucleotide corresponding to nucleotides 180–197 of intron 3 (relative to the A editing site) or position 1,414–1,439 of the 5-HT$_{2C}$R cDNA (exon 4)[24]. Polymerase chain reaction (PCR) amplification was used with the initial cDNA synthesis primer and a sense primer in exon 3 (position 1,063–1,080)[24]. Primer-extension analysis of RT-PCR reaction products was done for the A, C and D editing sites as described[10]. Primers for the A and C sites (Fig. 3a, b) corresponded to positions 1,136–1,153 and 1,143–1,160 (ref. 24), respectively, and were extended in the presence of either 1.2 mM deoxyadenosine 5′-triphosphate (dATP), 1.2 mM deoxycytosine 5′-triphosphate (dCTP), 5 mM dideoxyguanosine 5′-triphosphate (ddGTP) and 5 mM dideoxythymidine 5′-triphosphate (A-site) or 1.2 mM dATP, 1.2 mM dCTP, 1.2 mM deoxythymidine 5′-triphosphate and 5 mM ddGTP (C- and D-sites). For regional analysis of 5-HT$_{2C}$R expression (Fig. 4 and Table 1), reverse transcription was done using an antisense primer in exon 4 (positions 1,414–1,439); PCR amplification of cDNA was achieved using the initial cDNA synthesis primer and a sense primer (exon 3; positions 1,063–1,080)[24]. PCR reaction products derived from various brain regions, representing a pool of 5-HT$_{2C}$R cDNA isoforms, were analysed for editing by primer extension and by direct sequencing using *Taq* DNA polymerase and an antisense primer corresponding to positions 1,216–1,235 (refs 24). For the sequencing assay, products were separated on a 6% acrylamide–7M urea gel, generating a sequence ladder containing both A and G bands at positions corresponding to the A, B, C and D editing sites. The relative ratios of the A and G bands were quantified with a Molecular Dynamics phosphorimager. Four bands representing nucleotides that are not edited were chosen in both the A and G lanes and used to generate a factor for correction of differences in band intensity provided by differing deoxy/dideoxy nucleotide mixtures. Editing at the B site was consistently underestimated in this assay and sequence analyses of individual cDNA isolates (Table 1) indicated that the level of editing at the B position was similar to that seen at the A site.

***In vitro* editing/deamination assays.** Crude rat brain nuclear extracts were prepared as described[27] and resuspended in buffer A (25 mM HEPES (pH 7.9), 1 mM EDTA (pH 8.0), 10% glycerol, 1 mM dithiothreitol). Extracts were fractionated by cation-exchange column chromatography (Mono S; Pharmacia) and proteins were eluted using a linear gradient from 0 to 450 mM NaCl prepared by mixing buffers A and B (buffer A plus 1 M NaCl); 1-ml fractions were collected. NaCl concentrations in individual cation-exchange fractions were determined using a conductivity meter (Radiometer; Copenhagen). The control dsRNA substrate was transcribed from a 586-bp fragment of the α_{2A} adrenergic receptor (α_{2A}AR) subcloned into pBKSII$^-$ and linearized with either *Not*I or *Xba*I. Double-stranded α_{2A}AR RNA was produced by annealing single-stranded transcripts as described[10]. For synthesis of the 5-HT$_{2C}$R substrate, a 288-bp DNA fragment corresponding to positions −93 to +194 (relative to the A-site) was subcloned into pBKSII$^-$, linearized with *Xho*I, and transcribed with T7 RNA polymerase. For GluR-B, a 646-nucleotide DNA fragment corresponding to positions −256 to +390 (relative to the Q/R site) was subcloned into pBKSII$^-$, linearized with *Bam*HI, and transcribed with T3 RNA polymerase[10]. Production of inosine (adenosine deaminase activity) was determined by TLC of *in vitro* reaction products after incubation at 30 °C for 3 h in an assay (50 μl) containing 50 fmol of [α-^{32}P]ATP labelled RNA substrate (RNA specific activity, 2.2×10^8) and 15 μl fractionated rat brain extract in buffer A as described[10]; the final concentration of NaCl was adjusted in each fraction to either 150 or 115 mM for the α_{2A}AR and 5-HT$_{2C}$R RNA substrates, respectively. *In vitro* editing conditions were identical to those described for adenosine-deaminase assays except that the substrate RNAs were labelled with [α-^{32}P]uridine 5′-triphosphate (RNA specific activity, 2.2×10^6) to determine RNA concentration and the reaction products were analysed by primer extension or RT-PCR sequence analyses; the final concentration of NaCl was

adjusted in each fraction to either 115 or 100 mM for the 5-HT_{2C}R and GluR-B substrates, respectively.

Pharmacological characterization. For analysis of phosphoinositide hydrolysis, transfected cells were plated in DMEM medium containing 10% calf serum, penicillin and streptomycin; 24 h after electroporation, cells were labelled overnight with 2 μCi [^{3}H]myo-inositol/ml in serum-free, inositol-free DMEM. Before addition of 5-HT, cells were washed with serum-free medium and the accumulated ^{3}H-inositol monophosphate assayed[28]. Competition binding with [^{3}H]mesulergine (1 mM) (Fig. 3b) was done as described[29] and nonspecific binding was determined with 10 μM methysergide. Apparent K_i values were calculated according to ref. 30. Published 5-HT_{2C}R (INI) K_i values were used for clozapine, mesulergine, bromo-LSD and mianserin[29]. 1.6 μM PBZ decreased receptor density to 29.6% of control (Fig. 5c), as determined by saturation binding of [^{3}H]mesulergine. EC_{50}, E_{max} and B_{max} values ($n = 3$) for PBZ-treated INI and VSV isoforms were 6.6 ± 2.5 nM compared with 8.5 ± 3.7 nM, 320 ± 10 compared with 240 ± 20 per cent of basal, and 3,444 ± 448 compared with 946 ± 227 fmol per mg protein, respectively.

Received 22 August 1996; accepted 7 March 1997.

1. Hoyer, D. *et al.* IUP classification of receptors for 5-hydroxytryptamine (serotonin). *Pharmacol. Rev.* **46,** 157–203 (1994).
2. Polson, A. G., Bass, B. L. & Casey, J. L. RNA editing of hepatitis delta virus antigenome by dsRNA-adenosine deaminase. *Nature* **380,** 454–456 (1996).
3. Sommer, B., Kohler, M., Sprengel, R. & Seeburg, P. H. RNA editing in brain controls a determinant of ion flow in glutamate-gated channels. *Cell* **67,** 11–19 (1991).
4. Lomeli, H. *et al.* Control of kinetic properties of AMPA receptor channels by nuclear RNA editing. *Science* **266,** 1709–1713 (1994).
5. Kohler, M., Burnashev, N., Sakmann, B. & Seeburg, P. Determinants of Ca^{2+} permeabiity in both TM1 and TM2 of high affinity kainate receptor channels: diversity by RNA editing. *Neuron* **10,** 491–500 (1993).
6. Egebjerg, J. & Heinemann, S. F. Intron sequence directs RNA editing of the glutamate receptor subunit GluR2 coding sequence. *Proc. Natl Acad. Sci. USA* **90,** 755–759 (1993).
7. Zuker, M. Computer prediciton of RNA structure. *Meth. Enzymol.* **180,** 262–288 (1989).
8. Higuchi, M. *et al.* RNA editing of AMPA receptor subunit GluR-B: a base-paired intron–exon structure determines positon and efficiency. *Cell* **75,** 1361–1370 (1993).
9. Herb, A., Higuchi, M., Sprengel, R. & Seeburg, P. H. Q/R site editing in kainate receptor GluR5 and GluR6 pre-mRNAs requires distant intronic sequences. *Proc. Natl Acad. Sci. USA* **93,** 1875–1880 (1996).
10. Rueter, S. *et al.* Glutamate receptor RNA editing *in vitro* by enzymatic conversion of adenosine to inosine. *Science* **267,** 1491–1494 (1995).
11. Yang, J.H., Sklar, P., Axel, R. & Maniatis, T. Editing of glutamate receptor subunit B pre-mRNA *in vitro* by site-specific deamination of adenosine. *Nature* **374,** 77–81 (1995).
12. Maas, S. *et al.* Structural requirements for RNA editing in glutamate receptor pre-mRNAs by recombinant double-stranded RNA adenosine deaminase. *J. Biol. Chem.* **271,** 12221–12226 (1996).
13. Melcher, T. *et al.* A mammalian RNA editing enzyme. *Nature* **379,** 460–464 (1996).
14. Bass, B. RNA editing: New uses for old players in the RNA world. *The RNA World* 383–418 (Cold Spring Harbor Laboratory Press, New York, 1993).
15. Gomeza, J. *et al.* The second intracellular loop of metabotropic glutamate receptor 1 cooperates with the other intracellular domains to control coupling to G-proteins. *J. Biol. Chem.* **271,** 2199–2205 (1996).
16. Westphal, R. S., Backstrom, J. R. & Sanders-Bush, E. Increased basal phosphorylation of the constitutively active serotonin 2C receptor accompanies agonist-mediated desensitization. *Mol. Pharmacol.* **48,** 200–205 (1995).
17. Ariëns, E. J., Beld, A. J., Rodrigues de Miranda, J. F. & Simonis, A. M. *The Receptors* 33–91 (Plenum, New York, 1979).
18. Meller, E. *et al.* Receptor reserve for D2 dopaminergic inhibition of prolactin release *in vivo* and *in vitro*. *J. Pharmacol. Exp. Ther.* **257,** 668–675 (1991).
19. Leonhardt, S., Garospe, E., ,Hoffman, B. J. & Teitler, M. Molecular pharmacological differences in the interaction of serotonin with 5-hydroxytryptamine 1C and 5-hydroxytryptamine2 receptors. *Mol. Pharmacol.* **42,** 328–335 (1992).
20. Ross, E. M. G protein GTPase-activating proteins: regulation of speed, amplitude, and signaling selectivity. *Rec. Prog. Horm. Res.* **50,** 207–221 (1995).
21. Moro, O., Lameh, J., Högger, P. & Sadée, W. Hydrophobic amino acid in the i2 loop plays a key role in receptor–G protein coupling. *J. Biol. Chem.* **268,** 22273–22276 (1993).
22. Yu, L. *et al.* The mouse 5-HT1C receptor contains eight hydrophobic domains and is X-linked. *Mol. Brain Res.* **11,** 143–149 (1991).
23. Kennelly, P. J. & Krebs, E. G. Consensus sequences as substrate specificity determinants for protein kinases and protein phosphatases. *J. Biol. Chem.* **266,** 15555–15558 (1991).
24. Julius, D., MacDermott, A. B., Axel, R. & Jessell, T. M. Molecular characterization of a functional cDNA encoding the serotonin 1c receptor. *Science* **241,** 558–264 (1988).
25. Ausubel, F. *et al.* (eds) Current Protocols in Molecular Biology (Wiley, New York, 1989).
26. O'Connell, M. *et al.* Cloning of cDNAs encoding mammalian double-stranded RNA-specific adenosine deaminase. *Mol. Cell. Biol.* **15,** 1389–1397 (1995).
27. Gorski, K., Carneiro, M. & Schibler, U. Tissue-specific *in vitro* transcription from the mouse albumin promoter. *Cell* **47,** 767–776 (1986).
28. Barker, E. L., Westphal, R. S., Schmidt, D. & Sanders-Bush, E. Constitutively active 5-hydroxytryptamine2C receptors reveal novel inverse agonist activity of receptor ligands. *J. Biol. Chem.* **269,** 11687–11690 (1994).
29. Westphal, R. S. & Sanders-Bush, E. Reciprocal binding properties of 5-hydroxytryptamine type 2C receptor agonists and inverse agonists. *Mol. Pharmacol.* **46,** 937–942 (1994).
30. Cheng, Y. & Prusoff, W. H. Relationship between the inhibiton constant (K_i) and the concentration of inhibitor which causes 50 per cent inhibition (IC_{50}) of enzymatic reaction. *Biochem. Pharmacol.* **22,** 3099–3108 (1973).

Acknowledgements. We thank B. Wadzinski for assistance with biochemical fractionation analysis, J. Exton, J. Barnett and J. Patton for critical reading of this manuscript, and A. Westphal and A. Poindexter for their technical expertise. This work was supported by grants from the NIH, the National Defense Medical Center, Taipei, Taiwan, and the Pharmaceutical Manufacturers Association Foundation, Inc.

Correspondence and requests for materials should be addressed to R.B.E. (e-mail: ron.emeson@mcmail.vanderbilt.edu).

Elasticity and unfolding of single molecules of the giant muscle protein titin

L. Tskhovrebova*†, J. Trinick*, J. A. Sleep‡ & R. M. Simmons‡

* *Muscle Research Group, Department of Veterinary Clinical Science, Bristol University, Langford, Bristol BS18 7DY, UK*
‡ *MRC Muscle & Cell Motility Unit, Randall Institute, King's College London, 26–29 Drury Lane, London WC2B 5RL, UK*

The giant muscle protein titin, also called connectin, is responsible for the elasticity of relaxed striated muscle, as well as acting as the molecular scaffold for thick-filament formation[1,2]. The titin molecule consists largely of tandem domains of the immunoglobulin and fibronectin-III types, together with specialized binding regions and a putative elastic region, the PEVK domain[3]. We have done mechanical experiments on single molecules of titin to determine their visco-elastic properties, using an optical-tweezers technique. On a fast (0.1s) timescale titin is elastic and force–extension data can be fitted with standard random-coil polymer models, showing that there are two main sources of elasticity: one deriving from the entropy of straightening the molecule; the other consistent with extension of the polypeptide chain in the PEVK region. On a slower timescale and above a certain force threshold, the molecule displays stress-relaxation, which occurs in rapid steps of a few piconewtons, corresponding to yielding of internal structures by about 20 nm. This stress-relaxation probably derives from unfolding of immunoglobulin and fibronectin domains.

Relaxed striated muscle possesses markedly nonlinear visco-elastic properties, including stress-relaxation and hysteresis. The steady-state force–extension relationship is at first roughly exponential, but at extreme stretch there is a yield point, after which the curve is less steep. Elasticity derives principally from connections between the ends of thick filaments and the Z-line (Fig. 1a). These connections are formed by the I-band region of the roughly 3,000K protein titin; the end-to-end length of this region increases with muscle stretch, from about zero to 1 μm. The remaining (A-band) region of the titin molecule, 0.8 μm long, runs to the M-line and is normally integral with the thick filament. The maximum passive (yield) force per thick filament is in the range 100–200 pN, with between 3 and 6 titin molecules in each half filament, so the maximum force per molecule lies between 15 and 70 pN. The major part of skeletal muscle titin consists of 140–160 immunoglobulin domains and 132 fibronectin-III domains; in the I-band region the 1,000–2,200 residues of the so-called PEVK region are flanked by 70–90 immunoglobulin domains, depending on isoform[3]. Recent studies of epitope positions in preparations of stretched muscle fibres[4,5] suggest that titin has two physiologically important elastic mechanisms (Fig. 1b–d). At rest length, with no external force, the I-band region of the molecule probably assumes a random-coil configuration[6] (Fig. 1b). As the sarcomere is extended force begins to rise as the molecule is straightened, with little change in secondary or tertiary structure (Fig. 1c). With further stretch, force rises more steeply as the polypeptide conformation in the PEVK region changes from a compact to a more extended configuration (Fig. 1d). At extreme lengths titin detaches from the thick filament (yield point) and the A-band part of the molecule becomes extensible[7] (Fig. 1e). Whether the immunoglobulin or fibronectin

† Present address: Institute of Theoretical and Experimental Biophysics, Puschino, Moscow Region 142292, Russia.